Tribology International 200 (2024) 110075

Contents lists available at ScienceDirect

Tribology International

journal homepage: www.elsevier.com/locate/triboint

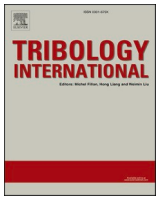

2D mica as a new additive for nanolubricants with high tribological performance

María J.G. Guimarey [a,b,*], Shadeepa Karunarathne [b], Chirag R. Ratwani [b], Jose Luis Viesca [b,c], A. Hernández Battez [b,c], Amr M. Abdelkader [b]

[a] Laboratory of Thermophysical and Tribological Properties, Nafomat Group, Department of Applied Physics, Faculty of Physics, University of Santiago de Compostela, 15782 Santiago de Compostela, Spain
[b] Department of Design and Engineering, Faculty of Science & Technology, Bournemouth University, Poole, Dorset BH12 5BB, United Kingdom
[c] Department of Construction and Manufacturing Engineering, University of Oviedo, Asturias, Spain

ARTICLE INFO

Keywords:
2D mica nanoadditives
Nanolubricants
Friction
Wear

ABSTRACT

This article presents 2D mica nanoplatelets as a novel additive to produce a stable engine lubricant. The planar structure and excellent mechanical properties of 2D mica contribute significantly to the improvements in tribological performance when evaluated under pure sliding and rolling/sliding contact configurations. The wear rate is reduced by 72 %, and the coefficient of friction (COF) decreases by 28 % when 2D mica is added to engine oil under pure sliding conditions. No tribological improvement was observed under rolling/sliding conditions. Our results also showed that nanosheet loading plays a significant role in nanolubricant performance, where 0.2 wt% is the optimum. These findings demonstrate superior performance to other 2D material nanoadditives and indicate the potential for commercial applications of 2D mica-based nanolubricants.

1. Introduction

Pursuing enhanced tribological performance in lubricants represents a pivotal area of contemporary materials science and engineering. Improving tribological properties is pertinent to numerous industrial sectors, including automotive, aerospace, manufacturing, and energy production [1]. As machinery becomes increasingly sophisticated and operates under more demanding conditions, the need for lubricants capable of reducing friction, minimizing wear, and enhancing efficiency becomes ever more pressing [2]. Consequently, developing novel lubricants with superior tribological properties has emerged as a focal point for researchers and engineers seeking to address the challenges posed by modern machinery [3].

A significant majority (87.9 %) of vehicles registered in the European Union (EU) in 2022 used internal combustion engines (ICEs) as the propulsion systems, as evidenced by data from the European Automobile Manufacturers' Association (ACEA) [4]. The continuous dominancy in the light-weight vehicle market by the vehicles with ICEs is highlighted here, and it is fair to anticipate that ICEs will maintain a substantial market presence in the coming years, making it imperative to advance ICE technology, particularly with regard to enhancing performance, reliability, and lifespan. The interaction between lubricant condition and tribological performance is pivotal in efficient ICE design of ICEs [5]. In order to extend their future market value, the current development of high-performance engine oils is tailored to outperform conventional lubricants [6]. As such, nanoadditives are a principal route to producing high-performance lubricants, particularly at high contact pressure and temperature.

Usually, engine oil comprises a base hydrocarbon oil along with an additive package. The most common additives are antiwear, antioxidants, dispersants, detergents, friction modifiers, viscosity modifiers, extreme pressure agents, anti-foaming agents and emulsifying compounds [7]. Zinc dialkyl dithiophosphate (ZDDP) is a popular additive for antiwear properties in engine oil applications. Nevertheless, concerns about the environmental impact of ZDDP, as well as its contribution to catalytic converter poisoning in automotive applications [8], have prompted research into alternative antiwear (AW) additives, including ashless AW additives [9], fluorinated ZDDP (F-ZDDP) [10,11], and ionic liquids [12].

Among the antiwear additives of interest, nanoparticles are currently

* Corresponding author at: Laboratory of Thermophysical and Tribological Properties, Nafomat Group, Department of Applied Physics, Faculty of Physics, University of Santiago de Compostela, 15782 Santiago de Compostela, Spain.
E-mail addresses: mgarciaguimarey@bournemouth.ac.uk, mariajesus.guimarey@usc.es (M.J.G. Guimarey).

https://doi.org/10.1016/j.triboint.2024.110075
Received 28 May 2024; Received in revised form 11 July 2024; Accepted 5 August 2024
Available online 5 August 2024

extensively studied as a potential alternative additive in commercial lubricants to meet the rising worldwide demand for high-performance lubricants. Apart from being environmentally friendly, nanoparticles offer numerous benefits, including enhanced durability, low volatility to withstand extreme temperatures, excellent thermal conductivity, and remarkable capability to minimize friction and wear [2]. Initially, metal oxide nanoparticles (e.g., Al_2O_3, TiO_2, Fe_3O_4) were introduced to enhance lubricant performance [13–15]. Their small size allows them to penetrate surface asperities, forming a protective layer. Their spherical shape allows them to perform a rolling effect that reduces friction and wear. Carbon-based nanoparticles (e.g., diamond, fullerene and graphene) emerged as promising additives due to their exceptional physicochemical properties as research progressed. Fullerene's spherical structure enables it to roll between surfaces, reducing frictional resistance, while graphene's 2D lattice structure provides remarkable mechanical, physical, and electrical properties [16]. These nanomaterials exhibit superior lubrication efficiency, forming robust tribofilms on surfaces, enhancing load-bearing capacity, and reducing energy losses [17].

A comparison of the various morphologies, typically spherical, sheet, granular, onion, and tube nanomaterials, reveals their distinct influence on the properties of nanolubricants [18]. Spherical shape nanoparticles typically showcase the rolling mechanism, acting as ball bearings between the contact surfaces. However, their tendency to agglomerate can compromise the stability and dispersibility of the fluid [3]. Nanoparticles with a sheet or lamellar-like structure include graphene [19], molybdenum disulfide (MoS_2) [20], boron nitride (BN) [21,22], and zirconium phosphate (ZrP) [23].

The ability of two-dimensional materials to slide along their surface, overcoming the weak van der Waals bonds, gives an added advantage in determining the tribological behaviour of these materials [24]. For example, with its 2D structure, graphene imparts exceptional mechanical strength and thermal conductivity to nanofluids, leading to enhanced load-carrying capacity and heat dissipation. Furthermore, graphene's large aspect ratio allows for improved dispersion and stability within the lubricant, ensuring uniform contact surface coverage [19]. The onion morphology with a complex two-part structure having an external spherical shape and an internal layered structure results in better tribological performance due to better stability. During its stable phase, it behaves like spherical morphology; however, in harsh conditions, it becomes sheet morphology by exfoliating [18]. Dai et al. [18] reported superior tribological performance of spherical, sheet, and onion morphologies compared to other morphologies.

2D materials offer several advantages over traditional additives for viscosity improvement and friction reduction. Their high surface area-to-volume ratio enhances their effectiveness at low concentrations. Their unique planar structure also allows them to penetrate surface asperities and form durable lubricating layers, leading to long-lasting friction reduction [25]. Recently, Alqahtani et al. [26] have investigated the tribological performance of 5W-30 engine oil with graphene nano-additives. These authors concluded that graphene nanoplatelet addition improved wear scar and coefficient of friction by 15 % and 33 %, respectively. Thachnatharen et al. [27] have studied the tribological behaviour of hexagonal boron nitride (hBN) as nanoadditives in SAE 20 W50 diesel engine oil using ASTM standard four-ball tribotester. The tribological results revealed 20.5 % and 9.47 % improvement in coefficient of friction (COF) and wear scar diameter (WSD) using hBN nanoadditives compared with bare engine oil. Yu et al. [28] analyzed different metal-organic frameworks (MOF) (metal ions: Ni^{2+}, Zn^{2+}, and Cu^{2+}) as lubricant additives in a 500 N base oil. The best tribological properties were obtained by adding 0.1 wt% Ni-MOF nanosheets, reducing friction by 33.2 % and wear by 98.7 % compared to pure oil. So, the most recent studies [26–32] have demonstrated that the incorporation of 2D materials not only improves the tribological properties and increases the viscosity of the lubricant [33] and its load-carrying capacity [34], but also that among all types of 2D materials, silicate-based nanosheets possess the advantages of abundant raw materials, are easy to exfoliate, and are relatively cost-effective [35]. Mica is a naturally occurring phyllosilicate mineral known for its excellent thermal stability, resistance against harsh oxidative conditions, and electrical insulation properties [36]. Its natural abundance makes it cost-effective compared to other 2D materials like graphene and hexagonal boron nitride (h-BN), making it a viable candidate for large-scale applications, is also environmentally friendly, offering an ecological alternative to other 2D materials. However, despite all these strengths, it has not been explored as a potential lubricant additive in tribology, with only a few publications on its use as a solid lubricant in coatings [35,37], even though the layered clay mineral of mica carries the capacity to be exfoliated along facets overcoming weak van der Waals forces upon the exposure to an external shear force, leading to excellent antiwear properties [37].

The authors note that there is a paucity of in-depth literature exploring motor oils' performance integrated with mica nanoparticles as lubricant additives. This knowledge is crucial for optimizing high-performance commercial oils that can be effectively and practically applied in the automotive field. Therefore, new approaches to enhancing the lubricative properties of engine oil (5W-30) were explored during the study through a more optimal viscosity behaviour and limiting friction and wear by incorporating 2D mica nanosheets as a lubricant additive. The results of nanolubricants with 2D materials were found to be promising, motivating the researchers to attempt a new member of the family.

2. Experimental details

2.1. Synthesis of mica nanosheets

Micronized mica flakes were purchased from Lingshou County Huayuan Mica Co. Ltd. Flakes were sieved with 325 mesh (44 μm). Collected particles were washed multiple times with Ethanol/ DI water mixture to remove the impurities and dried well before further processing. Through direct ultrasonication, micro-sized mica flakes (<45 μm) were transformed into mica nanosheets. In a typical experiment, 500 mg of mica was added to a mixture of 50 mL deionized water (DIW) and 50 mL ethanol (EtOH) and ultrasonicated at a frequency of 37 kHz for 12 h using a 220 W 2.8 L Ultrawave bath ultrasonicator. The ultrasonic exfoliation process was paused periodically to ensure that the temperature of the ultrasonication bath remained below 50 °C. The resulting suspension, which had a dark green-grey colour, was separated from the sedimented particles. The collected sample was sedimented by centrifuging at 1500 relative centrifugal force (RCF) for 30 min using a Sigma 1–16 K centrifuge. The resulting powder was dried in a vacuum oven for > 12 h at 120 °C, and the dehydrated mica nanosheets were kept in a sealed container until it's been added to the engine oil.

2.2. Characterization of mica nanosheets and engine oil

Mica nanosheets were characterized through a range of morphological and physicochemical characterization techniques. Transmission electron microscopy (TEM, JEOL 2010 and JEOL JEM-1400) was used to realize the exfoliated mica nanosheets' lateral dimensions and morphological properties. The mica nanosheet's layer thickness was studied using Atomic Force Microscopy (AFM- Park Systems XE 100). The surface elemental composition of 2D mica was analyzed through the energy dispersive X-ray spectroscopic analysis (EDS, EDAX Element EDS system), and the surface chemical composition was comprehended with the help of Fourier-transform infrared (FT-IR) spectroscopy (VARIAN 670-IR spectrophotometer) analysis. In addition, X-Ray diffraction analysis (XRD, Siemens D5000 diffractometer) was used to confirm the crystal phases present in the exfoliated layered structure.

The 2D mica-based nanolubricants were formulated using 5W-30 engine oil as the base lubricant. The properties of this engine oil were

measured using a Stabinger SVM 3000 viscometer (Anton Paar, Austria), which are summarized in Table 1. Further evaluation of engine oil properties was carried out with Raman microscopy during one of our previous studies [32], and the presence of characteristic peaks in two distinct wavenumber regions of the fingerprint region (800–1800 cm^{-1}) and high wavenumber region (2800–3500 cm^{-1}) attributing to the hydrocarbon structure of the oil was noticed during the study.

2.3. Nanolubricants preparation and stability assessment

The mica-based lubricants were prepared using the conventional two-step method. After exfoliation and vacuum drying, dry mica nanosheets were loaded at different mass loadings varying as 0.05, 0.1, 0.2, and 0.4 wt%, into the commercially purchased engine oil rated 5 W-30. Each nanolubricant was mixed by mechanical stirring (Fisherbrand Vortex) for 120 s and then further dispersed with the help of an ultrasonic bath sonicator (FB11203, 37 kHz, Fisher Scientific, USA) operated for 4 h. The stability of the prepared nanolubricants was analyzed using a refractometer (Mettler Toledo RA-510 M) following a previously reported experimental procedure [38]. This was used to observe the changes in the refractive index (n) over the period of 96 hrs. (temporal evolution of n).

2.4. Measurement of viscosity index and kinematic viscosity

Guidelines outlined in ASTM D7042–04 and ASTM D2270–04 standards were followed during the viscosity index (VI) and kinematic viscosity assessments of all mica-based lubricants, which were assessed and computed using the SVM 3000 Anton Paar rotational Stabinger viscometer. Kinematic viscosity measurements were conducted at temperatures of 40 °C and 100 °C.

2.5. Sliding tests

The samples from both naked engine oil and the mica-dispersed nanolubricant were performed in the sliding test experiment using a ball-on-three-pins tribometer (T-PTD200) integrated within a rheometer (Anton Paar MCR 302) under rotational motion.

The test specimens (ball and pins) were made with high-quality AISI 52100 grade steel with a hardness of 62–66 on Rockwell scale (HRC), 190–210 GPa of Young modulus and 0.29 of Poisson ratio. The chemical composition of the AISI 52100 grade steel specimens is gathered in Table 2. In terms of dimensions, the balls were 12.7 mm in diameter, while the pins had a diameter and height of 6 mm, and the surface roughness (R_a) of both specimens was 0.15 μm and 0.3 μm, respectively. A volume of 1 mL sample lubricant was used for the sliding test, and the temperature was maintained at 120 °C throughout the experiment. During the test, 9.43 N of a normal force, resulting in a maximum Hertzian pressure of 1.11 GPa was applied, and the ball surface velocity was maintained at 0.1 m/s with 213 rpm of a rotational speed, acquiring a total sliding distance of 3400 m. Each experiment was triplicated, and the mean coefficient of friction (COF) was computed for each nanolubricant and the engine oil, along with its standard deviation.

Well-cleaned specimens were used for every test through ultrasonic cleaning in petroleum ether for 5 mins, rinsing with ethanol, and drying with hot air from the blower in respective order. For further details on this tribometer configuration, please refer to previous publications. [39,40].

Table 2
Chemical composition (wt%) of AISI 52100 grade steel.

Material	C	Cr	Mn	Si	P	S
AISI 52100	0.98 – 1.10	1.30 – 1.60	0.25 - 0.45	0.15 – 0.35	≤0.025	≤0.025

2.6. Worn surface analysis

A 3D confocal profilometer (Sensofar, S-Neox) was used to analyze roughness and the wear that occurred at the surface of pins after the sliding tests. SEM and EDX surface analysis techniques were used to analyze the morphological features in the wear surface. Possible wear mechanisms were also identified. Further, the potential formation of tribofilms on the surface of worn steel films was studied using a Confocal Raman microscopy (WITec alpha300R+).

2.7. Rolling/sliding tests

Tribological properties under different lubrication regimes of the as-prepared nanolubricants were analyzed using a MTM2 (Mini Traction Machine from PCS Instruments) tribometer, which was configured as a ball-on-disc setup. Stribeck curves were generated for the nanolubricants at various temperatures, ranging from 40 °C to 120 °C. The tests employed a slide-to-roll ratio (SRR) of 50%, a load of 50 N (resulting in a maximum contact pressure of 1.15 GPa), and an average entrainment speed varying between 2500 and 10 mm/s. Each test utilized a volume of 10 mL of lubricant. The balls with 19.05 mm diameter and disks with 46 mm diameter were used for the test with the hardness of the respective specimens were 800–920 HV and 720–780, respectively, while both specimens were made out of AISI 52100 steel with surface roughness Ra ≤ 0.02 μm. Before testing, the specimens underwent a 5-minute ultrasonic cleaning process in a heptane-filled ultrasonic bath, followed by drying with hot air.

3. Results and discussion

3.1. Characterization of the engine oil and the mica nanosheets

The size of the mica nanosheets was measured using TEM, and the results are presented in Fig. 1. The images in Fig. 1a-b show multi-layer mica sheets with a lateral dimension of approximately 200–300 nm. The non-contact AFM image presented in Fig. 1c confirms that the mica nanosheets were well-exfoliated, with a layer thickness of < 10 nm. EDX analysis (Fig. 1d) confirms the presence of Si, Al, K, Fe, Mg, and O in the nanosheet structure, which are key elements in biotite mica. XRD spectra presented in Fig. 1e further verified the presence of biotite, as the diffraction pattern is well-aligned with the previous indexing on JCPDS 02–1297 for biotite mica [41]. With the positioning of the (002) plane at 27.4°, the interlayer distance can be calculated as 0.32 nm following Bragg's law, knowing the samples were exposed to X-rays with 1.54 Å wavelength. In addition, Fig. S1 presents XRD spectra of bulk mica. The diffraction peak strengths of bulk mica and mica nanosheets were compared with the peak strength of NaCl, which was mixed with an equal weight percentage. Fig. S1 indicates a significant reduction of the peak strength in mica nanosheets, suggesting a successful physical cleavage of mica layers. Further, the overlapping of peak positions in mica nanosheets and bulk mica and a similar elemental composition of

Table 1
Characteristics of the pure 5W-30 engine oil.

5W-30	Provider	Nature	Density (20 °C) / kg m^{-3}	Kinematic Viscosity (40 °C) / mm^2 s^{-1}	Kinematic Viscosity (100 °C) / mm^2 s^{-1}	Viscosity Index (VI)
	TOTAL ESPAÑA SAU.	Synthetic	845.7	56.8	10.2	172

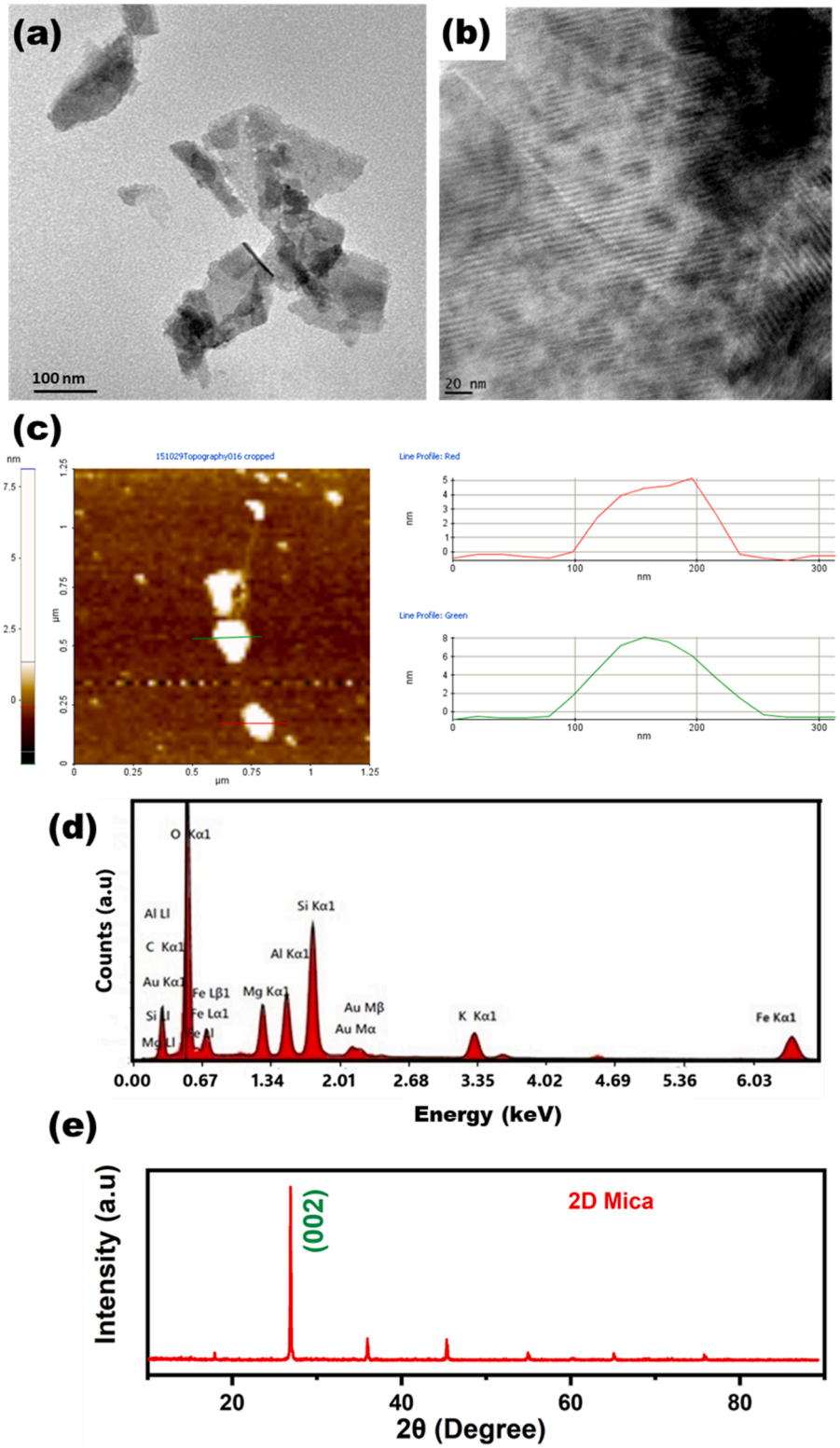

Fig. 1. a, b) TEM images, c) AFM, d) EDX, and e) XRD of multi-layer exfoliated mica sheets.

mica micro flakes (see Fig. S2, Supplementary Material) to mica nanosheets imply that no chemical modifications occurred during the ultrasonication-assisted exfoliation process. Fig. 2 depicts the FT-IR spectra of the mica nanosheets. In which, multiple characteristic peaks were identifiable at 962 cm^{-1}, 752 cm^{-1}, and 671 cm^{-1} attributed to ν(Si-O-Si), ν(Al-O-A), and ν(Si-O-Si), respectively [42]. An additional peak presented at 1639 cm^{-1} is owing to adsorbed moisture [43].

3.2. Nanolubricants stability

It is essential to have a long-term stable suspension of mica nanosheets in the engine oil to deliver prolonged lubricative activities. The stability of the mica-based nanolubricants was evaluated through continuous monitoring of the refractive index. The change in the refractive index (n) over time is presented in Fig. 3 for the naked engine

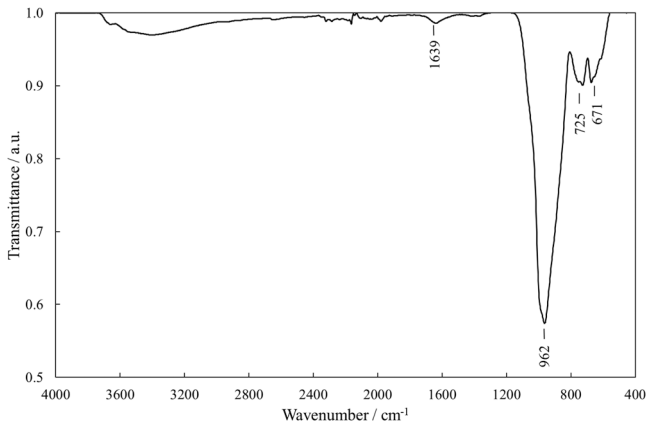

Fig. 2. FT-IR spectrum of mica nanosheets.

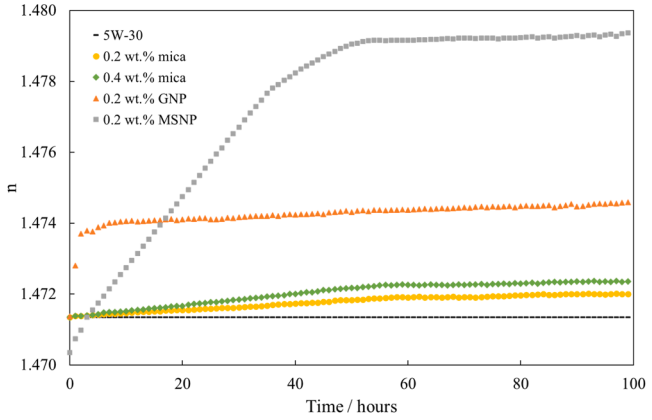

Fig. 3. Refractive index (n) evolution over time at 20 °C of the: 5 W-30 engine oil (broken line), 0.2 wt% (circle) mica-based nanolubricants, and 0.4 wt% (rhombus), and GNP (triangle)- and MSNP (square)-based nanolubricants at 0.2 wt% [39].

oil and the nanolubricants containing the highest concentrations of mica loading (0.2 and 0.4 wt%) samples over a period of 4 days (96 h). The results confirm that the mica-based nanolubricants were well-dispersed. The refractive index of the base oil ($n = 1.47135$) increased by 0.0007 with the addition of 0.2 wt% mica into the oil. As the 2D mica loading increased to 0.4 wt%, the refractive index further increased ($n = 1.47236$) by 0.001. The stabilities achieved for the 2D mica-based nanolubricants were higher than those previously reported for the same engine oil (5 W-30) with graphene nanoplatelets (GNP) and molybdenum disulfide nanosheet additives (MSNP). The time-dependent variation of the refractive index was reported as 0.008 and 0.003 over 96 h for the 0.2 wt% loaded graphene nanoplatelets and molybdenum disulfide nanosheet-based nanolubricants, respectively [39].

3.3. Kinematic viscosity and viscosity index

The difference in kinematic viscosity between the mica-based nanolubricants (ν_{nl}) and the neat engine oil (ν_{fo}) is expressed as $\left(\frac{\nu_{fo}-\nu_{nl}}{\nu_{fo}}\right) \times 100$, and Fig. 4a presents its behaviour against the varying temperature and nanoadditive loading. The addition of 2D mica resulted in the reduction of the kinematic viscosity of the oil. The kinematic viscosity decreased as the mica content of the nanolubricants increased, except for the highest concentration of nanolubricants (0.4 wt%). The observed phenomenon may be attributed to the self-aggregation of 2D mica nanoparticles at higher loading. Although the dispersion was stable at room temperature, with relatively higher oil viscosity, it could not withstand higher temperatures under reduced oil viscosity and surface tension, causing 2D mica to aggregate and reducing the effective loading of the particles. The kinematic viscosity decreased by 5%, 10%, 13%, and 8% for the mica-based nanolubricants with 0.05 wt%, 0.1 wt%, 0.2 wt%, and 0.4 wt%, respectively, compared to the virgin engine oil. The self-lubricating nature of mica nanosheets is assumed to trigger this reduction in kinematic viscosity, where shear forces cause layers to slide against each other. Therefore, adding the appropriate amount of mica to the formulated oil can reduce internal friction during fluid flow. This is similar to improvements achieved with other 2D materials and layered nanoplatelets from our previous works [39]. Fig. 4a shows that the variation of the kinematic viscosity with nanoadditive loading was similar at both 40 °C and 100 °C.

Fig. 4b illustrates the VI of the 5W-30 engine oil (0 wt%) and the newly formulated nanolubricants. The data reveal a decrease in VI by 2.3%, 4.1%, 4.7%, and 2.9% for the 0.05 wt%, 0.1 wt%, 0.2 wt%, and 0.4 wt% mica concentrations, respectively, relative to the pure engine oil. These observations confirm the influence of the 2D mica in lowering the VI of the base oil. However, it is noteworthy to mention that these reductions are all less than 5%. This ensures that the nanolubricant maintains its effectiveness at elevated temperatures by preserving the depth of the oil film. The lower VI can be attributed to a higher viscosity variation observed between 40 °C and 100 °C for the mica-based nanolubricants compared to the engine oil. Pourpasha et al. have previously reported on this phenomenon. [44].

3.4. Sliding tests

Fig. 5 exhibits the COF obtained by performing the sliding test at

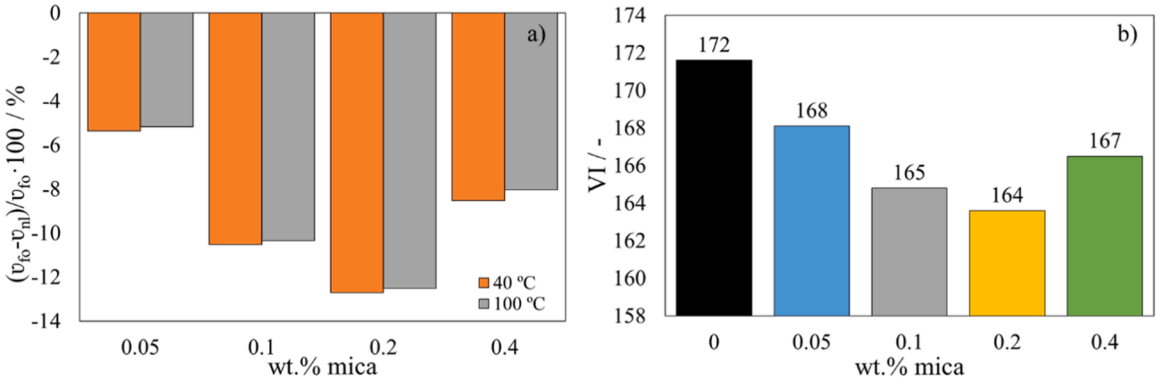

Fig. 4. a) Average relative variation of the mica-based nanolubricant viscosity (ν_{nl}) with respect to the formulated oil (ν_{fo}) at 40 °C and 100 °C, and b) viscosity index, VI, for all the mica-based nanolubricants.

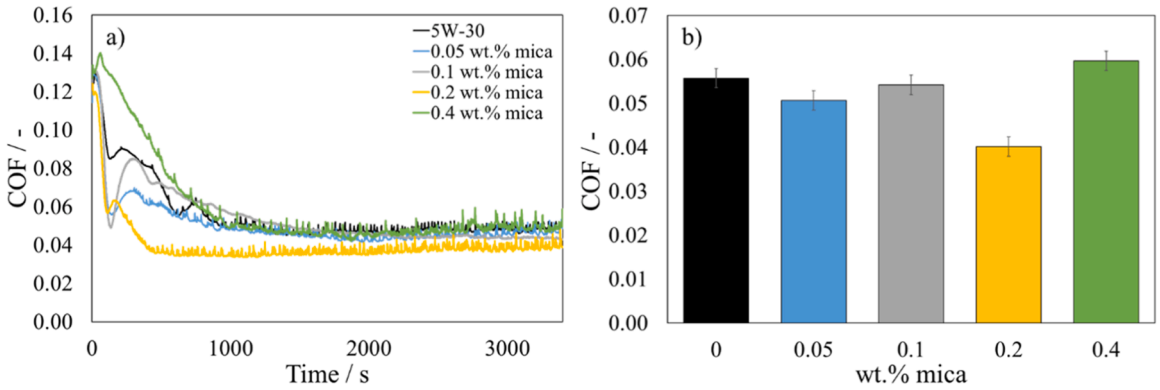

Fig. 5. Sliding friction results: a) temporal evolution of coefficient of friction (COF) and b) average COF for trials with each lubricant sample.

120 °C for pure engine oil and formulated engine oil samples with several loadings of mica nanosheets. The temporal evolution of COF is shown in Fig. 5a, revealing that nanolubricants significantly reduced the COF, except for the highest nanolubricant concentration (0.4 wt%). During the first 1000 s of the sliding friction test (engine start), all lubricants, again with the exception of the highest 2D mica loading, showed a typical behaviour of a sharp decrease in COF in the first minute of sliding, followed by an increase to a second peak and then a gradual decrease to a time-independent plateau. This two-step COF reduction has also been observed with other friction modifiers, such as organic friction modifiers (OFMs) [45]. The optimal 2D mica loading was determined to be 0.2 wt% with an average COF reduction of 28%. The nanolubricants with 0.05 wt% and 0.1 wt% mica loading reduced the average COF by only 9% and 3%, respectively. Beyond the optimum concentration (0.2 wt%), the likelihood of agglomeration of the mica nanosheets increased (as shown in Fig. 3), resulting in the formation of larger clusters that can disrupt the establishment of a uniform protective film. This agglomeration leads to a decrease in the effectiveness of the lubricant, as the larger clusters are less effective in reducing friction and wear. For instance, research on MoS_2 nanomaterials and other nanosheet-based lubricants highlights similar issues with concentration-dependent agglomeration, emphasizing the importance of optimizing nanoparticle concentration to maintain stability and performance in tribological applications [20]. In agreement with the provided explanation, 0.4 wt% mica-based nanolubricant resulted in a slight increase in COF (around 7%) relative to the COF obtained for the base engine oil. These results are consistent with those obtained for kinematic viscosity and VI (Figs. 4a and 4b), where the trend of viscosity reduction does not hold at higher nanoadditive loads.

Fig. 6a shows the wear variation with the four mica-based nanolubricants in contrast to the one with the pure engine oil based on the wear properties, including wear scar diameter (WSD), wear track depth (WTD), and wear area measurements. All the mica-based nanolubricants reduced the wear parameters compared to the 5W-30 engine oil. It can be noted that the highest reduction for the three wear parameters can be achieved with the 0.2 wt% mica nanolubricant, which showed about 27%, 35%, and 49% reduction for WSD, WTD, and worn area, respectively. High mica loading (0.4 wt%) resulted in an increase in wear parameters, reaching an increase of 5%, 11% and 15% for WSD, WTD and wear area over the 5W-30 engine oil. Thus, the wear analysis revealed that the ideal concentration of mica nanoadditive for antiwear performance is 0.2 wt%. Several authors have reported the existence of an optimum concentration when nanoparticles are used as lubricant additives [46]. Again, the higher loaded nanolubricant (0.4 wt%) resulted in a deterioration of the antiwear performance of the engine oil. The clusters formed above a certain concentration, which favours the agglomeration of the nanosheets, can also act as abrasive particles, increasing friction and wear [47–49].

The wear rate (W*R*) was calculated from the wear volume measurements in the steel pins using the following equation [50,51]:

$$W = \frac{\Delta V}{F_n S_s} \tag{1}$$

where W is the specific wear rate ($mm^3 \cdot N^{-1} \cdot m^{-1}$), ΔV is the volume loss (mm^3), F_n is the applied load (N), and S_s is the sliding distance (m).

Fig. 6b demonstrates the effect of mica nanoadditive loading on the wear rate. Incorporating 2D mica nanoparticles at a concentration of 0.2 wt% resulted in a significant enhancement in wear resistance against the pure engine oil, exhibiting a maximum enhancement of 72%. These wear characteristics align with previously collected wear parameter data (Fig. 6a). Fig. 6 illustrates the relationship between the presence of mica nanoadditives and the antiwear performance of the 5W-30 engine

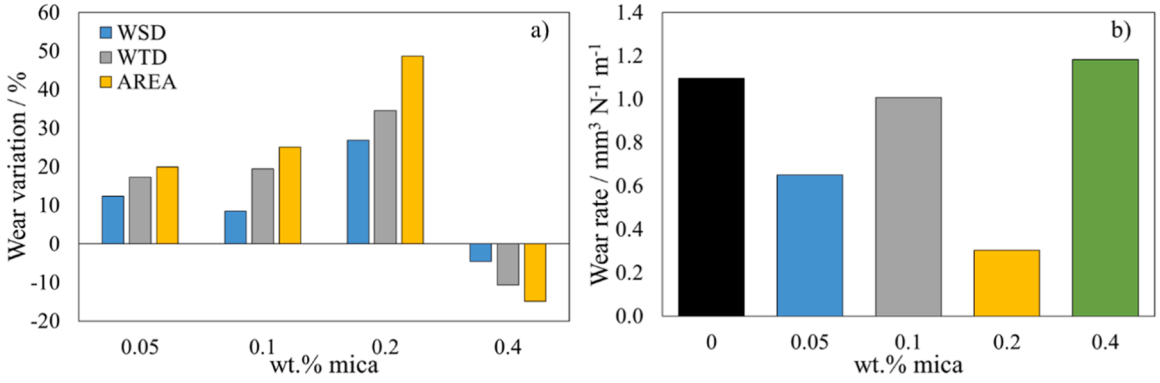

Fig. 6. a) Wear variation for wear scar diameter (WSD), wear track depth (WTD) and worn area with the mica-based nanolubricants compared to the engine oil, and b) wear rate results with all the lubricant samples.

oil, which is correlated with variations in the coefficient of friction (COF) (Fig. 5b). At a mica loading of 0.4 wt%, the highest wear area and wear rate values were observed, coinciding with the highest COF value.

The tribological results of this study were compared to those previously reported [39] lubricant additives like graphene and molybdenum disulfide nanosheets at 0.05, 0.10, and 0.20 wt% in 5W-30 engine oil. The test was conducted under the same contact configuration, with a maximum Hertzian contact pressure of 1.11 GPa and a load test condition of 20 N. However, the temperature and sliding distance were different, at 363.15 K and 180 m, respectively. Under optimal conditions, the average COF reduction obtained for MSNP-enhanced oil was 5.9%, almost 5 times lower than the optimum 2D mica concentration (28% at 0.2 wt%) achieved in this study.

In regards to antiwear performance, the engine oil showed the highest reduction in wear area with GNP and MSNP concentrations at 0.20 wt%, reaching 22% and 13%, respectively [39]. However, these reductions in wear area are less than 50% of those achieved in this study with the optimal concentration of 2D mica nanoadditives. Therefore, it can be concluded that mica nanoadditives exhibit significantly superior tribological performance compared to previously reported nanoadditives in the literature. This makes the 2D mica suitable as a lubricant additive for formulated oils, improving their tribological and viscous performance. Previous research [52,53] demonstrated that adding layered materials to friction surfaces could cause interlayer sliding, which significantly reduces the COF and wear rate.

3.5. Worn surface analysis

To elucidate the impact of the nanoadditives on tribological performance and identify potential wear mechanisms associated with the 2D mica nanoparticles, 3D optical profilometry was employed to quantify the cross-sectional profiles of the wear tracks generated on the steel pins. Fig. 7 presents the roughness profiles of the wear scars treated with the 5W-30 engine oil and the four formulated nanolubricants. The analysis revealed that the cross-sectional area of the wear track lubricated with the nanolubricant containing 0.2 wt% mica (yellow line) exhibited minimal wear depth compared to all other lubricants tested. This observation aligns with the previously measured friction and wear rate data, where the 0.2 wt% mica loading demonstrated the most effective antifriction and antiwear properties. Conversely, the nanolubricant formulated with 0.4 wt% mica displayed the greatest wear track cross-sectional area compared to the engine oil. This finding again corroborates the prior tribological results in Figs. 5b and 6b. It can be concluded that the abrasive nature of mica can be advantageous up to a specific concentration. However, exceeding this critical point leads to the formation of mica agglomerates, which contribute to a phenomenon known as third-body abrasion. This phenomenon ultimately results in increased friction and wear. These observations highlight the significance of identifying the optimal concentration of the nanoadditives to achieve the most beneficial tribological performance.

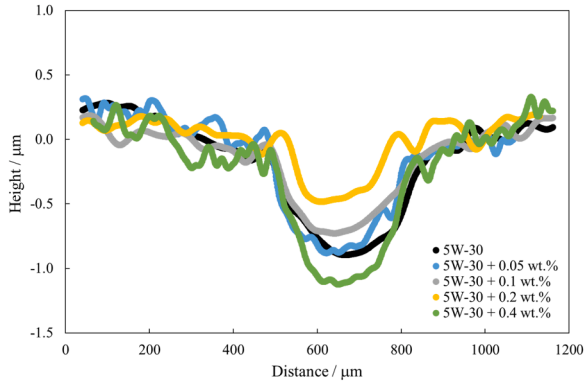

Fig. 7. Cross-section profiles of wear tracks lubricated with 5W-30 engine oil and with mica-based nanolubricants.

The arithmetic mean surface roughness (R_a) measured from the profile cross-section inside the wear scars was calculated using SensoMap software and the ISO 4287 standard with the subsequent equation:

$$R_a = \frac{1}{L}\int_0^L Z(x)dx \tag{2}$$

where L is the evaluation length, Z(x) is the profile height function, and R_a is the arithmetic mean of the absolute values of the profile height deviations from the mean line recorded within the evaluation length.

The arithmetic mean height (S_a) also was calculated using SensoMap software and the ISO 25178 standard with the following equation:

$$S_a = \frac{1}{A}\iint Z(x,y)dxdy \tag{3}$$

Table 3 summarizes the average roughness and height parameters for the worn surfaces lubricated with the engine oil and the mica-based nanolubricants. The results indicate that the mica nanoadditives do not have a polishing effect, as R_a increases for wear scars lubricated with the mica-based nanolubricants compared to those lubricated with engine oil. The R_a values increase by 1.2, 0.5, 2.2, and 0.9 times for the wear track lubricated with the 0.05, 0.1, 0.2, and 0.4 wt% mica-based nanolubricant, respectively, in contrast to the surface directly lubricated with the pure 5 W-30 engine oil. The S_a results for the wear scars lubricated with 5 W-30 engine oil and four different mica-based nanolubricant concentrations reveal that at 0.2 wt%, the S_a value decreased to 129 nm compared with the baseline value for the 5 W-30 engine oil (142 nm), indicating better dispersion and more effective formation of a uniform protective film, reducing the surface roughness. However, at 0.4 wt%, the S_a value significantly increased to 269 nm. This indicates substantial agglomeration, resulting in larger clusters that disrupt the uniform protective film, leading to higher surface roughness and reduced effectiveness as a lubricant. To provide a more comprehensive analysis, Fig. S3 (available in the Supplementary Material) shows the 3D surface topography images for the wear track lubricated with the engine oil and the mica-based nanolubricants.

The impact of mica nanoadditives on the mechanism for wear was additionally explored through electron microscopy examination of the wear surfaces. Images 8a, c, and e depict the wear scar of the AISI 52100 steel pin, serving as the lower specimen, under lubrication with the 5W-30 engine oil at three distinct magnifications (500X, 1000X, and 5000X). The wear reduction produced for the optimum concentration (0.2 wt%) of 2D mica-based nanolubricant is clearly more pronounced, as demonstrated in Fig. 8b. The wear scar diameter reduces to less than half when 2D mica is added to the 5W-30 engine oil. The sliding friction tests performed with both lubricants show abrasive wear on the wear scar (Fig. 8e and f). However, the surface lubricated with 0.2 wt% 2D mica loading revealed the presence of wear debris on the worn area, suggesting a possible deposit of mica during the sliding friction test. This was confirmed by the EDX elemental analysis of the marked areas in Figs. 8c and 8d. Table 4 provides a summary of the EDX findings from the elemental spectroscopic study conducted on the steel pins subsequent to the sliding friction test employing both 5W-30 engine oil and the ideal concentration of 2D mica-based nanolubricant (0.2 wt%). The EDX analysis on the wear surface lubricated with the 5W-30 engine oil detected the elements present in the steel (Fe, C and Cr) and the tribolayer formed by the reaction of the AW/EP additive, which are ZDDP (Zn, P, S) [32]. The EDX analysis on the wear surface lubricated with the 0.2 wt% mica nanolubricant confirmed the presence of Si, Al, K, Fe, Mg and O, elemental composition of biotite mica nanoparticles. Despite the low concentration of 2D mica nanoadditive used, traces of these compounds can be detected, especially the presence of O, Mg and K, which are not detected on the wear track lubricated with the 5W-30 engine oil without nanoadditives. This fact could be explained by the deposition of

Table 3
Arithmetic mean roughness surface (R_a) and arithmetic meah height (S_a) and their standard deviation were measured on the wear scar of the steel pin after tests with all the lubricant samples.

5W-30		0.05 wt%		0.1 wt%		0.2 wt%		0.4 wt%	
R_a/nm	σ/nm	R_a/nm	σ/nm	R_a/nm	σ/nm	R_a/nm	σ/nm	R_a/nm	σ/nm
10.2	5.2	22	13	15.3	7.3	33	16	19	12
S_a/nm	σ/nm	S_a/nm	σ/nm	S_a/nm	σ/nm	S_a/nm	σ/nm	S_a/nm	σ/nm
142	50	173	58	141	42	129	41	269	41

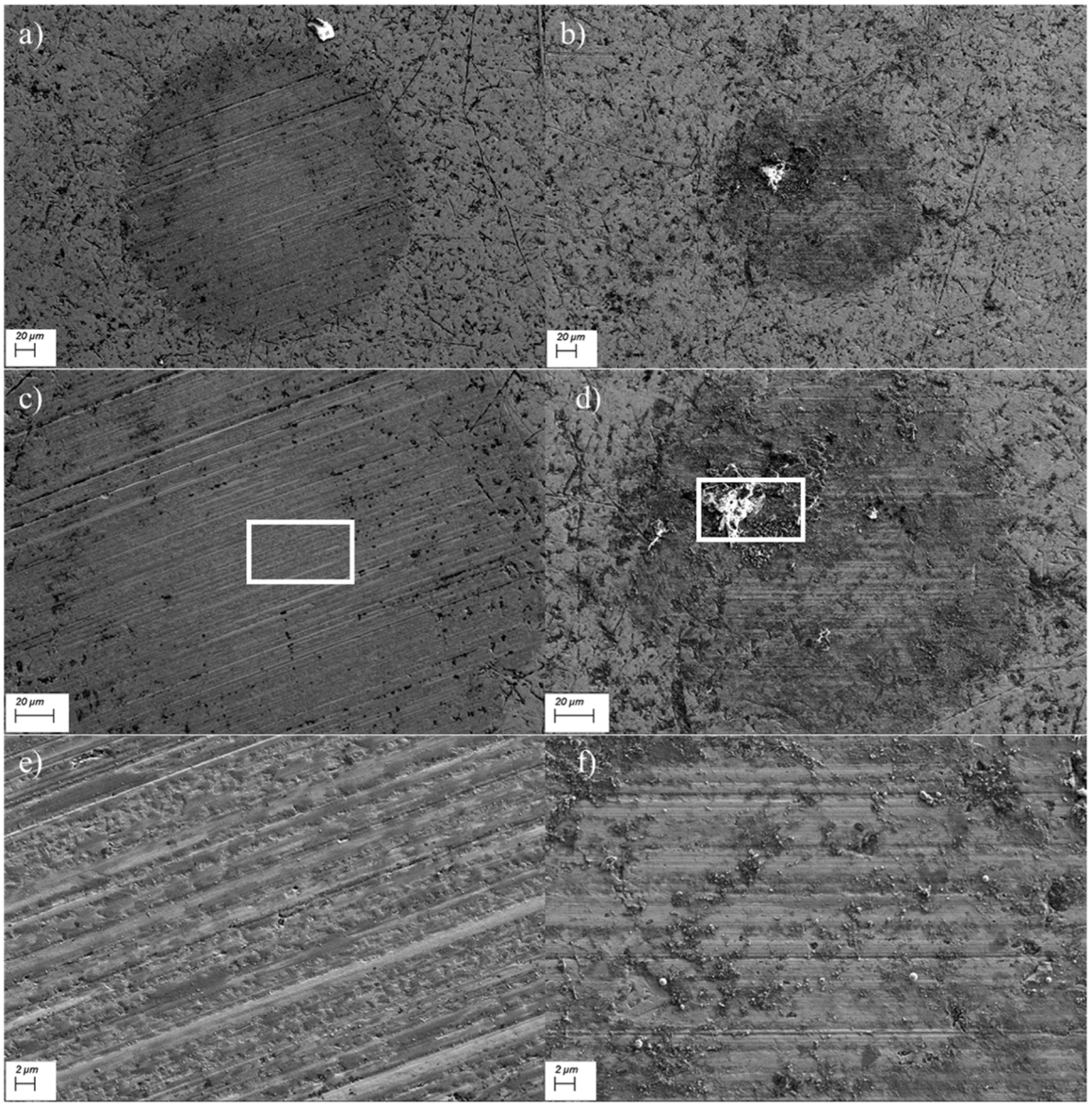

Fig. 8. SEM micrographs showing the wear scars on the steel pins from the sliding friction test with: (a, c, e) pure 5W-30 engine oil and (b, d, f) 0.2 wt% mica-based nanolubricant.

Table 4
EDX elemental analysis (wt%) on the wear scar.

Lubricant	C	Ni	O	Na	Mg	Al	Si	P	S	Cl	K	Ca	Cr	Mn	Fe	Zn	Total
5W−30	4.6	-	-	-	-	0.3	0.4	0.3	0.4	-	-	0.1	1.4	-	92.2	0.3	100.0
0.2 wt% mica	32.7	2.3	13.4	0.6	0.2	0.4	0.2	0.2	0.3	0.4	0.1	0.1	0.8	0.2	47.7	0.4	100.0

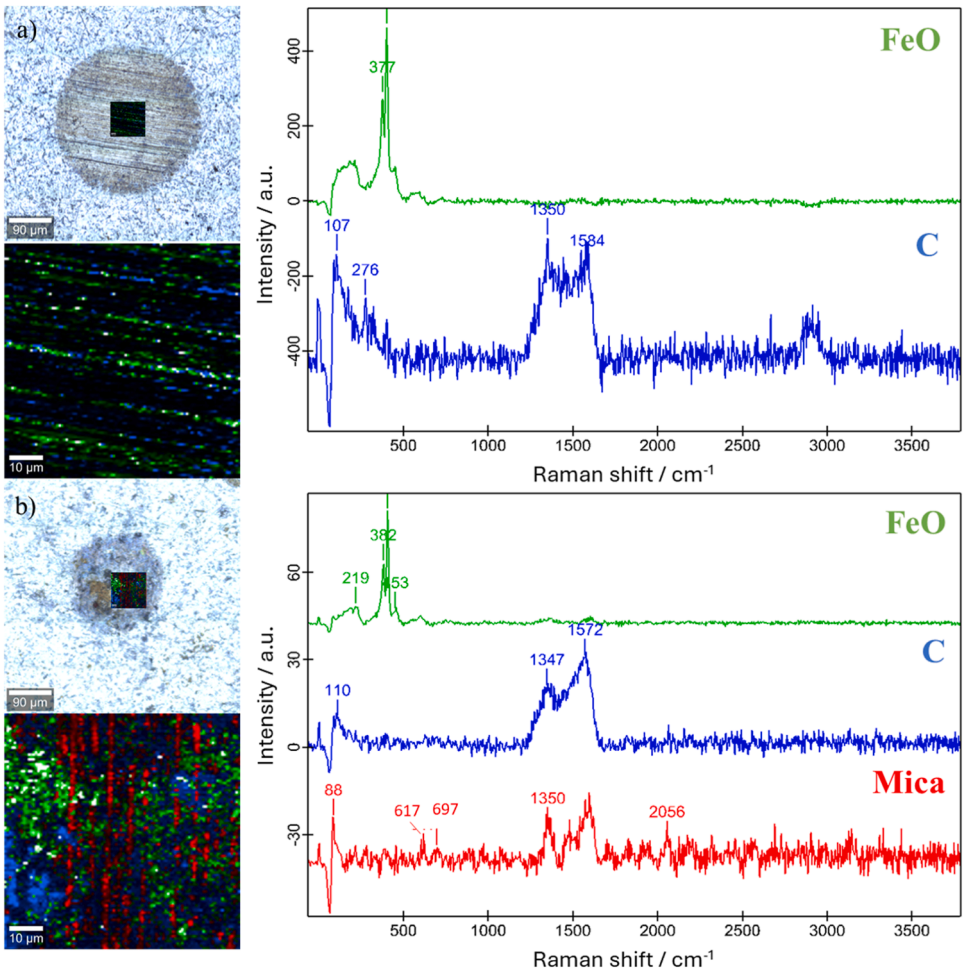

Fig. 9. Raman spectroscopy mapping of the wear surface treated with a) engine oil and b) the optimum mica-based nanolubricant.

2D mica nanoparticles during the sliding friction test.

After conducting sliding tests on the steel pin's surface, Raman spectroscopy and elemental mapping analyses were performed to investigate the potential influence of nanoparticles in the contact region. Fig. 9a and Fig. 9b depict the Raman mapping of the tribofilms produced using the commercial engine oil and the 0.2 wt% mica-containing nanolubricant, respectively. The results indicate the presence of prominent peaks at approximately 219 and 380 cm^{-1}, which are indicative of hematite (α-Fe_2O_3). Within the range of 1300 to 1600 cm^{-1}, two distinct bands, D and G, indicate the presence of carbon structures formed on steel surfaces via the decomposition of hydrocarbon radicals from the oil [54]. The Raman mapping of the wear track lubricated by 5W-30 engine oil shows the presence of iron oxides and carbon structures (green and blue areas) in the sliding direction. Both components are detected lodged in the grooves longitudinally. The iron oxides are formed as a result of the high contact pressure applied during the friction tests. In the wear track lubricated with the 2D mica nanolubricant, the Raman spectrum displays characteristic bands at 617 and 697 cm^{-1}, which are assigned to vibrations related to δ(Si–O–Si), typical of biotite mica [43]. The wear surface shows that the biotite mica (red zone) is lodged in the grooves, creating a tribofilm that reduces contact between the ball and the pin, resulting in reduced friction and wear. The use of mica-based nanolubricants resulted in the formation of a tribofilm and increased surface roughness on the wear tracks.

3.6. Rolling/sliding tests

Fig. 10 illustrates the Stribeck curves for both the engine oil and nanolubricants across various temperatures (40, 60, 80, 100, and 120 °C), maintaining a SSR of 50% and a load of 50 N. As the speed varies from low to high speeds under all temperatures, the 5W-30 oil and all nanolubricants transitioned from mixed lubrication (mL) to elasto-hydrodynamic (EHL) regime, as expected. The study found that the traction performance of mica nanolubricants remained consistent across various concentrations of mica nanoadditives within the EHL regime. Despite the promising tribological performance observed with the 2D mica nanolubricants, their COF under ML conditions did not surpass that of the commercial engine oil. Additionally, the increase in the COF was not proportional to the concentration of 2D mica in the nanolubricant at lower temperatures (40 °C, 60 °C, and 80 °C). For instance, when tested at 10 mm/s and 40 °C, the COF increased by 30%, 43%, 40%, and 12% for the 0.05, 0.1, 0.2, and 0.4 wt% mica nanolubricants, respectively, compared to the 5W-30 oil. The addition of mica nanoadditives to the engine oil may lead to the formation of agglomerates or clusters of mica nanoparticles within the lubricant, which could explain the increase in COF under the ML regime. The presence of clusters of nanoparticles may cause uneven distribution or deposition on the contacting surfaces, resulting in localized areas of increased friction. Furthermore, the use of 2D mica nanoparticles can modify the surface topography and chemical interactions between the lubricated surfaces, which may lead to increased asperity contact and friction. This is supported by the results of the surface roughness analysis on the wear tracks (see Table 3). At lower temperatures, the viscosity of the lubricant is higher (Table 1). Higher viscosity can impede the flow of the lubricant and make it more challenging to form an effective boundary layer between the rubbing surfaces. In such conditions, the presence of mica nanosheets becomes

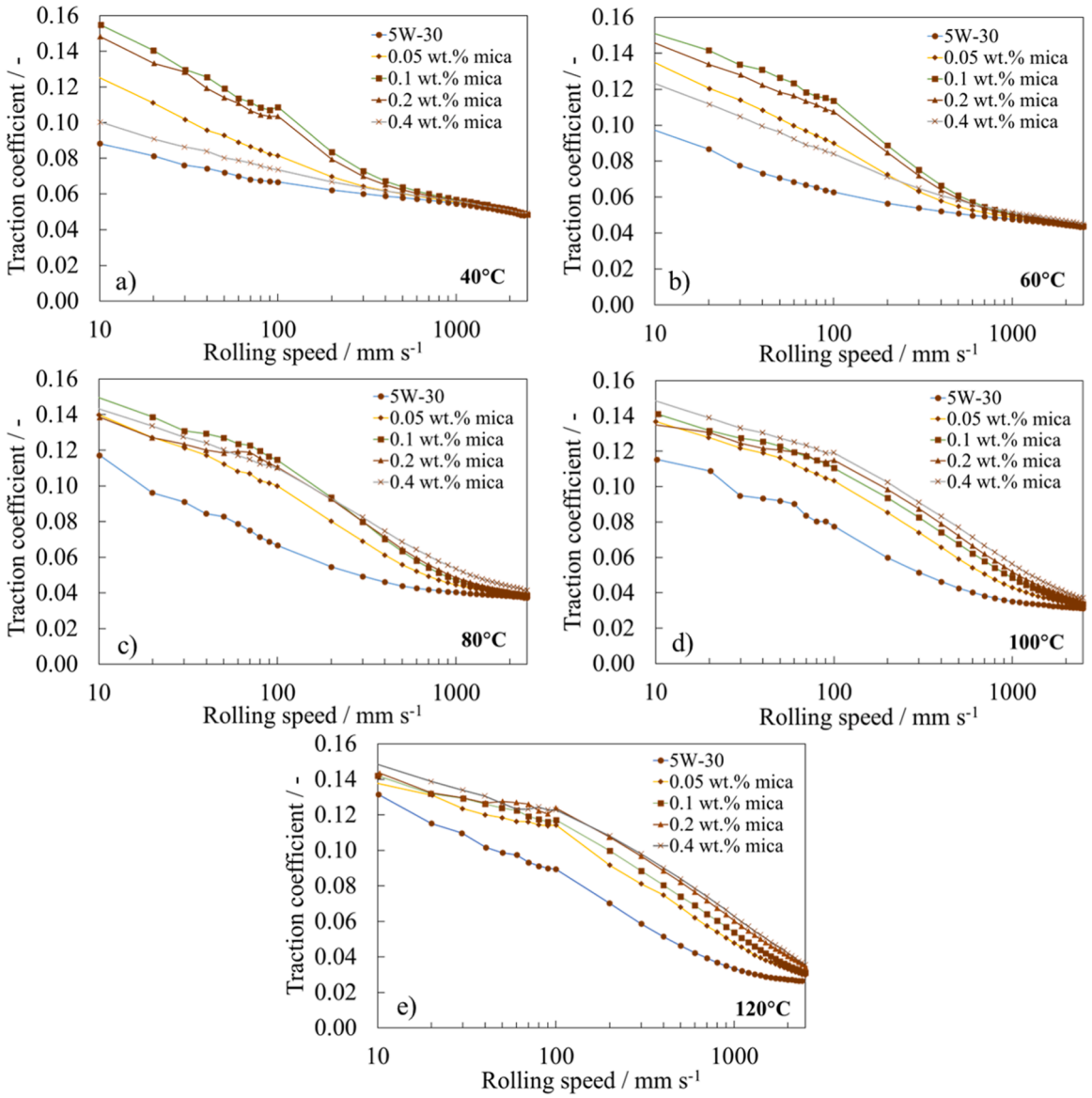

Fig. 10. Stribeck curves of the engine oil and the mica-based nanolubricants (different concentrations) at various temperatures from the rolling/sliding friction tests.

more pronounced in reducing direct metal-to-metal contact and thus lowering friction. When present in higher concentrations, mica nanosheets can form a more continuous boundary layer between the rubbing surfaces. This phenomenon may be indicative of the lower increase in COF observed at 0.4 wt% mica content relative to lower concentrations at low temperatures.

4. Conclusions

This paper investigated using 2D mica as nanoadditives for engine lubricants. The study yielded several significant findings. Firstly, incorporating mica nanosheets into SAE 5W-30 improved the thermophysical characteristics of the resulting nanolubricant. A significant reduction in kinematic viscosity was observed, with the most pronounced effect being observed at 0.2 wt% loading. Secondly, sliding friction tests demonstrated a notable decrease in COF and wear rate at the optimized loading of mica nanoadditives (0.2 wt%), achieving 28% and 72% reductions, respectively. Thirdly, analyses using roughness measurements, SEM, EDS, and Raman spectroscopy revealed the formation of tribofilms facilitated by mica nanoadditives. Finally, assessments conducted under rolling/sliding conditions showed increased COF for all mica-based nanolubricants in the mixed lubrication regime. This increase may be attributed to the formation of clusters within the lubricant due to an excess of the concentration of the nanoadditives. Therefore, optimizing the concentration of mica-based nanolubricants according to the specific tribological contact conditions will be necessary for their industrial use.

Statement originality

There is no conflict of interest exists in the submission of this manuscript. I would like to declare on behalf of my co-authors that the work described was original research that has not been published previously, and not under consideration for publication elsewhere, in whole or in part.

CRediT authorship contribution statement

María Jesús García Guimarey: Writing – review & editing, Writing – original draft, Methodology, Investigation, Formal analysis, Conceptualization. **Amr M. Abdelkader:** Writing – review & editing, Supervision, Conceptualization. **Chirag R. Ratwani:** Writing – review &

editing, Methodology, Conceptualization. **Shadeepa Karunarathne:** Writing – review & editing, Methodology, Conceptualization. **Antolín Hernández Battez:** Writing – review & editing, Supervision, Formal analysis, Conceptualization. **Jose Luis Viesca:** Writing – review & editing, Supervision, Formal analysis, Conceptualization.

Declaration of Competing Interest

The authors declare that they have no known competing financial interests or personal relationships that could have appeared to influence the work reported in this paper.

Data availability

Data will be made available on request.

Acknowledgements

The authors thank the following institutions and grants for supporting this research: Xunta de Galicia (ED431C 2020/10) and MCIN/AEI/10.13039/501100011033 through the PID2020-112846RB-C22 project. Additionally, Dr. MJGG acknowledges the Xunta de Galicia (Spain) for the postdoctoral fellowship (reference ED481D 2023/016).

Appendix A. Supporting information

Supplementary data associated with this article can be found in the online version at doi:10.1016/j.triboint.2024.110075.

References

[1] Singh A, Chauhan P, Mamatha TG. A review on tribological performance of lubricants with nanoparticles additives. Mater Today Proc 2020;25:586–91. https://doi.org/10.1016/j.matpr.2019.07.245.
[2] Ali ZAAA, Takhakh AM, Al-Waily M. A review of use of nanoparticle additives in lubricants to improve its tribological properties. Mater Today Proc 2022;52:1442–50. https://doi.org/10.1016/j.matpr.2021.11.193.
[3] Jason YJJ, How HG, Teoh YH, Chuah HG. A study on the tribological performance of nanolubricants. Processes 2020;8:1372. https://doi.org/10.3390/pr8111372.
[4] ACEA: New EU car sales by power source. ACEA figures; 2022. In: 2023.
[5] Agocs A, Besser C, Brenner J, Budnyk S, Frauscher M, Dörr N. Engine oils in the field: a comprehensive tribological assessment of engine oil degradation in a passenger car. Tribol Lett 2022;70:28. https://doi.org/10.1007/s11249-022-01566-7.
[6] Liu H, Liu H, Zhu C, Parker RG. Effects of lubrication on gear performance: a review. Mech Mach Theory 2020;145:103701. https://doi.org/10.1016/j.mechmachtheory.2019.103701.
[7] Nagy AL, Knaup JC, Zsoldos I. Investigation of used engine oil lubricating performance through oil analysis and friction and wear measurements. Acta Tech Jaurinensis 2019;12:237–51. https://doi.org/10.14513/actatechjaur.v12.n3.495.
[8] Lin YC, So H. Limitations on use of ZDDP as an antiwear additive in boundary lubrication. Tribol Int 2004;37:25–33. https://doi.org/10.1016/S0301-679X(03)00111-7.
[9] Kim B, Jiang JC, Aswath PB. Mechanism of wear at extreme load and boundary conditions with ashless anti-wear additives: analysis of wear surfaces and wear debris. Wear 2011;270:181–94. https://doi.org/10.1016/j.wear.2010.10.058.
[10] Mourhatch R, Aswath PB. Tribological behavior and nature of tribofilms generated from fluorinated ZDDP in comparison to ZDDP under extreme pressure conditions—part 1: structure and chemistry of tribofilms. Tribol Int 2011;44:187–200. https://doi.org/10.1016/j.triboint.2010.10.018.
[11] Mourhatch R, Aswath PB. Tribological behavior and nature of tribofilms generated from fluorinated ZDDP in comparison to ZDDP under extreme pressure conditions—part II: morphology and nanoscale properties of tribofilms. Tribol Int 2011;44:201–10. https://doi.org/10.1016/j.triboint.2010.10.035.
[12] Zhou Y, Qu J. Ionic liquids as lubricant additives: a review. ACS Appl Mater Interfaces 2017;9:3209–22. https://doi.org/10.1021/acsami.6b12489.
[13] Luo T, Wei X, Huang X, Huang L, Yang F. Tribological properties of Al_2O_3 nanoparticles as lubricating oil additives. Ceram Int 2014;40:7143–9. https://doi.org/10.1016/j.ceramint.2013.12.050.
[14] Zhang L, Chen L, Wan H, Chen J, Zhou H. Synthesis and tribological properties of stearic acid-modified anatase (TiO_2) nanoparticles. Tribol Lett 2011;41:409–16. https://doi.org/10.1007/s11249-010-9724-z.
[15] Guimarey MJG, Liñeira del Río JM, Fernández J. Improvement of the lubrication performance of an ester base oil with coated ferrite nanoadditives for different material pairs. J Mol Liq 2022;350:118550. https://doi.org/10.1016/j.molliq.2022.118550.
[16] Zhao J, Mao J, Li Y, He Y, Luo J. Friction-induced nano-structural evolution of graphene as a lubrication additive. Appl Surf Sci 2018;434:21–7. https://doi.org/10.1016/j.apsusc.2017.10.119.
[17] Eswaraiah V, Sankaranarayanan V, Ramaprabhu S. Graphene-based engine oil nanofluids for tribological applications. ACS Appl Mater Interfaces 2011;3:4221–7. https://doi.org/10.1021/am200851z.
[18] Dai W, Kheireddin B, Gao H, Liang H. Roles of nanoparticles in oil lubrication. Tribol Int 2016;102:88–98. https://doi.org/10.1016/j.triboint.2016.05.020.
[19] Berman D, Erdemir A, Sumant A. Graphene: a new emerging lubricant. Mater Today 2014;17:31–42. https://doi.org/10.1016/j.mattod.2013.12.003.
[20] Lu Z, Lin Q, Cao Z, Li W, Gong J, Wang Y, et al. MoS_2 nanomaterials as lubricant additives: a review. Lubricants 2023;11:527. https://doi.org/10.3390/lubricants11120527.
[21] Wang L, Han W, Ge C, Zhang R, Bai Y, Zhang X. Covalent functionalized boron nitride nanosheets as efficient lubricant oil additives. Adv Mater Interfaces 2019;6:1901172. https://doi.org/10.1002/admi.201901172.
[22] Guimarey MJG, Ratwani CR, Xie K, Koohgilani M, Hadfield M, Kamali AR, et al. Multifunctional steel surface through the treatment with graphene and h-BN. Tribol Int 2023;180:108264. https://doi.org/10.1016/j.triboint.2023.108264.
[23] He X, Xiao H, Choi H, Díaz A, Mosby B, Clearfield A, et al. α-Zirconium phosphate nanoplatelets as lubricant additives. Colloids Surf A Physicochem Eng Asp 2014;452:32–8. https://doi.org/10.1016/j.colsurfa.2014.03.041.
[24] Spear J, Ewers B, Batteas J. 2D-nanomaterials for controlling friction and wear at interfaces. Nano Today 2015;10:301–14. https://doi.org/10.1016/j.nantod.2015.04.003.
[25] Xiao H, Liu S. 2D nanomaterials as lubricant additive: a review. Mater Des 2017;135:319–32. https://doi.org/10.1016/j.matdes.2017.09.029.
[26] Alqahtani B, Hoziefa W, Abdel M 1 am HM, Hamoud M, Salunkhe S, Elshalakany AB, et al. Tribological performance and rheological properties of engine oil with graphene nano-additives. Lubricants 2022;10:137. https://doi.org/10.3390/lubricants10070137.
[27] Thachnatharen N, Khalid M, Arulraj A, Sridewi N. Tribological performance of hexagonal boron nitride (hBN) as nano-additives in military grade diesel engine oil. Mater Today Proc 2022;50:70–3. https://doi.org/10.1016/j.matpr.2021.04.145.
[28] Yu H, Liu X, Meng W, Zheng Z, Qiao D, Feng D, et al. Synthesis of ultrathin two-dimensional metal-organic framework nanosheets for lubricant additives. Mater Des 2022;223:111251. https://doi.org/10.1016/j.matdes.2022.111251.
[29] Sidh KN, Jangra D, Hirani H. An experimental investigation of the tribological performance and dispersibility of 2D nanoparticles as oil additives. Lubricants 2023;11:179. https://doi.org/10.3390/lubricants11040179.
[30] Nagarajan T, Sridewi N, Wong WP, Walvekar R, Khalid M. Enhanced tribological properties of diesel-based engine oil through synergistic MoS_2-graphene nanohybrid additive. Sci Rep 2023;13:17424. https://doi.org/10.1038/s41598-023-43260-1.
[31] Dassenoy F. Nanoparticles as additives for the development of high performance and environmentally friendly engine lubricants. Tribol Online 2019;14:237–53. https://doi.org/10.2474/trol.14.237.
[32] Guimarey MJG, Viesca JL, Abdelkader AM, Thomas B, Hernández Battez A, Hadfield M. Electrochemically exfoliated graphene and molybdenum disulfide nanoplatelets as lubricant additives. J Mol Liq 2021;342:116959. https://doi.org/10.1016/j.molliq.2021.116959.
[33] Li J, Chen D, Sun K, Pan R, Tang Y. Molecular dynamics simulation and experimental study of the rheological performance of graphene lubricant oil. Diam Relat Mater 2024;141:110721. https://doi.org/10.1016/j.diamond.2023.110721.
[34] Chen D, Sun Y, Sun K, Fan J. Computational fluid dynamics-based investigation of the static and dynamic characteristic of hydrostatic bearing with nanolubricant: a theoretical method. In: Proceedings of the Institution of Mechanical Engineers, part E: journal of process mechanical engineering 2023:2234–43. https://doi.org/10.1177/09544089221133658.
[35] Oshita K, Yanagi M, Okada Y, Komiyama S. Tribological properties of a synthetic mica-organic intercalation compound used as a solid lubricant. Surf Coat Technol 2017;325:738–45. https://doi.org/10.1016/j.surfcoat.2017.01.080.
[36] Gan D, Lu S, Song C, Wang Z. Mechanical properties and frictional behavior of a mica-filled poly(aryl ether ketone) composite. Eur Polym J 2001;37:1359–65. https://doi.org/10.1016/S0014-3057(01)00010-6.
[37] Oshita K, Komiyama S, Sasaki S. Preparation of a mica–organic hybrid solid lubricant and characterization of its lubrication mechanisms. Tribol Int 2018;123:349–58. https://doi.org/10.1016/j.triboint.2018.03.017.
[38] Guimarey MJG, Comuñas MJP, López ER, Amigo A, Fernández J. Thermophysical properties of polyalphaolefin oil modified with nanoadditives. J Chem Thermodyn 2019;131:192–205. https://doi.org/10.1016/j.jct.2018.10.035.
[39] Guimarey MJG, Abdelkader AM, Comuñas MJP, Alvarez-Lorenzo C, Thomas B, Fernández J, et al. Comparison between thermophysical and tribological properties of two engine lubricant additives: electrochemically exfoliated graphene and molybdenum disulfide nanoplatelets. Nanotechnology 2020;32:025701. https://doi.org/10.1088/1361-6528/abb7b1.
[40] Liñeira del Río JM, Alba A, Guimarey MJG, Prado JI, Amigo A, Fernández J. Surface tension, wettability and tribological properties of a low viscosity oil using $CaCO_3$ and CeF_3 nanoparticles as additives. J Mol Liq 2023;391:123188. https://doi.org/10.1016/j.molliq.2023.123188.
[41] Kalita JM, Wary G. Effect on thermoluminescence parameters of biotite mineral due to thermal quenching. J Lumin 2012;132:2952–6. https://doi.org/10.1016/j.jlumin.2012.06.009.

[42] Zhao W, Xu Y, Song C, Chen J, Liu X. Polyimide/mica hybrid films with low coefficient of thermal expansion and low dielectric constant. e-Polym 2019;19:181–9. https://doi.org/10.1515/epoly-2019-0019.
[43] Singh M, Singh L. Vibrational spectroscopic study of muscovite and biotite layered phyllosilicates. Indian J Pure Appl. Phy 2016;54:116–22. ⟨https://doi.org/10.56042/ijpap.v54i2.8521⟩.
[44] Pourpasha H, Zeinali Heris S, Mahian O, Wongwises S. The effect of multi-wall carbon nanotubes/turbine meter oil nanofluid concentration on the thermophysical properties of lubricants. Powder Technol 2020;367:133–42. https://doi.org/10.1016/j.powtec.2020.03.037.
[45] Spikes H. Friction modifier additives. Tribol Lett 2015;60:1–26. https://doi.org/10.1007/s11249-015-0589-z.
[46] Waqas M, Zahid R, Bhutta MU, Khan ZA, Saeed A. A review of friction performance of lubricants with nano additives. Materials 2021;14:6310. https://doi.org/10.3390/ma14216310.
[47] Ali I, Basheer AA, Kucherova A, Memetov N, Pasko T, Ovchinnikov K, et al. Advances in carbon nanomaterials as lubricants modifiers. J Mol Liq 2019;279:251–66. https://doi.org/10.1016/j.molliq.2019.01.113.
[48] Jin B, Chen G, He Y, Zhang C, Luo J. Lubrication properties of graphene under harsh working conditions. Mater Today Adv 2023;18:100369. https://doi.org/10.1016/j.mtadv.2023.100369.
[49] Opia AC, Hamid MKA, Syahrullail S, Johnson CAN, Rahim AB, Abdulrahman MBJE. Nano-particles additives as a promising trend in tribology: a review on their fundamentals and mechanisms on friction and wear reduction. Evergreen 2021;8:777–98. https://doi.org/10.5109/4742121.
[50] Zawawi N, Azmi W, Redhwan A, Mohd Zaki S. Coefficient of friction and wear rate effects of different composite nanolubricant concentrations on Aluminium 2024 plate. IOP Conf Ser Mater Sci Eng 2017;257:012065. https://doi.org/10.1088/1757-899X/257/1/012065.
[51] Motamen Salehi F, Morina A, Neville A. The effect of soot and diesel contamination on wear and friction of engine oil pump. Tribol Int 2017;115:285–96. https://doi.org/10.1016/j.triboint.2017.05.041.
[52] Chouhan A, Mungse HP, Khatri OP. Surface chemistry of graphene and graphene oxide: a versatile route for their dispersion and tribological applications. Adv Colloid Interface Sci 2020;283:102215. https://doi.org/10.1016/j.cis.2020.102215.
[53] Sahu J, Panda K, Gupta B, Kumar N, Manojkumar PA, Kamruddin M. Enhanced tribo-chemical properties of oxygen functionalized mechanically exfoliated hexagonal boron nitride nanolubricant additives. Mater Chem Phys 2018;207:412–22. https://doi.org/10.1016/j.matchemphys.2017.12.050.
[54] Guo H, Lou C, Pang J, Bellomo V, Mantegna N, Iglesias P. Linear alkylbenzenesulfonate-based protic ionic liquids: physicochemical properties and tribological performance as lubricant additives to a non-polar base oil. J Mol Liq 2022;361:119535. https://doi.org/10.1016/j.molliq.2022.119535.